Vol. 18, No. 1 (2019) 361-373
Revista Mexicana de Ingeniería Química

SYNTHESIS OF A GEOPOLYMER AND USE OF RESPONSE SURFACE METHODOLOGY TO OPTIMIZE THE BOND STRENGTH TO RED BRICK FOR IMPROVING THE INTERNAL COATING IN BURNER KILNS

SÍNTESIS DE UN GEOPOLÍMERO Y USO DE LA METODOLOGÍA DE SUPERFICIE DE RESPUESTA PARA OPTIMIZAR SU ADHERENCIA EN LADRILLO ROJO PARA SU USO COMO RECUBRIMIENTO INTERNO EN HORNOS LADRILLEROS

J.A. Torres-Ochoa[1,4], N.R. Osornio-Rubio[1,2], H. Jiménez-Islas[3], J.L. Navarrete-Bolaños[3], G.M. Martínez-González[1*]

[1]*Departamento de Ingeniería Química,* [2]*Departamento de Ingeniería Ambiental,* [3]*Departamento de Ingeniería Bioquímica, Tecnológico Nacional de México en Celaya. Antonio García Cubas Pte #600 esq. Av. Tecnológico. Celaya, Gto. México. C.P. 38010.*

[4]*CINVESTAV-Unidad Querétaro, Libramiento Norponiente No. 2000. C. P. 78230, Querétaro, México.*

Received: October 15 2018; Accepted: November 20, 2018

Abstract

In Mexico, fixed kilns made of red brick after several burn cycles at 1000 °C, may expand, crack and open. In light of that, we worked to obtain a geopolymer using clays (Caolín, Tepozán and Bauwer), that attaches to red brick. The clays were characterized using energy dispersive X-ray spectroscopy (EDS), atomic absorption spectroscopy (AAS), UV-VIS spectrophotometry and powder X-ray diffraction (PXRD), finding that the clays have refractory properties. The response surface methodology was used to optimize the adherence of the geopolymer on red brick, keeping the sodium silicate concentration constant. The optimal formulation of the geopolymer contains 50% commercial sodium silicate, 21% Caolín, 23% Tepozán, and 6% Bauwer, where the curing time was 7 days and the burning cycle was 8 h at 1000 °C. The best fit was achieved with a quadratic model that predicts an adherence of 3.2 MPa, comparable to the experimental value of 2.8 MPa. The geopolymer can be used as an internal coating in brick kilns to increase its useful life. In addition, the geopolymer has potential use as a coating for materials for refractory use.

Keywords: Geopolymer, sodium silicate, refractory clays, design of experiments, response surface, brick kilns.

Resumen

En México, los hornos fijos de ladrillo rojo después de varios ciclos de combustión a 1000 °C, se pueden expandir, agrietar y abrir, por lo que en este trabajo se obtuvo un geopolímero usando arcillas (Caolín, Tepozán y Bauwer), que se adhiere al ladrillo rojo. Las arcillas se caracterizaron utilizando espectroscopia de rayos X de energía dispersiva (EDS), espectroscopia de absorción atómica (AAS), espectrofotometría UV-VIS y difracción de rayos X en polvo (PXRD), encontrando que las arcillas tienen propiedades refractarias. La metodología de superficie de respuesta se utilizó para optimizar la adherencia del geopolímero sobre ladrillo rojo, manteniendo constante la concentración de silicato sódico. La formulación óptima del geopolímero contiene 50% de silicato sódico comercial, 21% de Caolín, 23% de Tepozán y 6% de Bauwer, donde el tiempo de curado fue de 7 días y el ciclo de quemado fue de 8 h a 1000 °C. El mejor ajuste se logró con un modelo cuadrático que predice una adherencia de 3.2 MPa, comparable con el valor experimental de 2.8 MPa. El geopolímero se puede utilizar como recubrimiento interno en hornos ladrilleros para aumentar su vida útil. Además, el geopolímero tiene uso potencial como recubrimiento de materiales para uso refractario.

Palabras clave: geopolímero, silicato de sodio, arcillas refractarias, diseño de experimentos, superficie de respuesta, hornos ladrilleros.

* *Corresponding author. E-mail*: gloriam@iqcelaya.itc.mx
Tel. +52 (461) 611-75-75 Ext. 5580.
doi: https://doi.org/10.24275/uam/izt/dcbi/revmexingquim/2019v18n1/TorresO
issn-e: 2395-8472

1 Introduction

Currently, there is an increasing demand for building new homes, buildings and public spaces. Thus, the construction industry requires resources and raw materials to satisfy these requirements, leading to high demand for concrete, steel, glass, red brick, geopolymers, and other materials. The cement industry is a major source of carbon dioxide emissions leading to environmental damage and global warming.

As such, better alternatives to the use of Portland cement-based concrete are needed; these alternatives must have high strength and durability as well as low cost and ease of preparation. A large number of studies have put forth new derived geopolymer materials with strength and durability similar to conventional concrete (Mehta and Siddique, 2016; Ankur and Rafat, 2016). The geopolymer products and their adherence, malleability and physical and chemical properties depend on the raw materials and processing conditions (Duxson *et al*., 2007).

Some studies have developed cement-free cementing materials, bonded with cementitious materials called alkaline-activated binders (more commonly known as geopolymers). Different types of raw materials are used to form alkaline-activated materials, such as furnace waste, metakaolin, ash and red mud. Materials containing SiO_2 generate geopolymers of excellent quality based on their mechanical properties. The state of the art in this field showed that this type of material is ecologically friendly as an alternative to ordinary Portland cement (Faris *et al*., 2017). There are multiple geopolymer applications, including reinforcing Portland cement with a montmorillonite aggregate with high amounts of SiO_2. This cement has great importance for the construction industry (Chang *et al*., 2007).

Compounds have been synthesized at room temperature by mixing metakaolin with potassium silica solution and clay-based ceramic, and test results show that the particle size affects the mechanical strength during thermal exposure at 1000 °C. The results showed that the highest content of fine particles below 90 μm and gradual distribution of other fractions from 150 to 710 μm led to improved stability during thermal exposure. Potassium-based geopolymers reinforced with fine particles have a flexural strength of 12 MPa and a compression strength of 90 MPa, in both their initial state and after exposure to 1000 °C (Kovárik *et al*., 2017).

Using geopolymers to preserve stone monuments is a proposed method for the construction of monument replicates *in situ*. This technique has been applied to historical monuments to observe their decay when exposed to several factors such as environmental contamination (Perez-Monserrat *et al*., 2013; Clausi *et al*., 2016; Yun-Ming *et al*., 2016). A water/clay ratio of 1:3 was found to improve the physical, mechanical and adsorption properties in geopolymeric products, maximizing their cadmium adsorption capacity from wastewater (Alshaaer *et al*., 2016). SEM and EDS analyses show that Al and Si favor the formation of a geopolymer structure, and test results support their potential application in sedimentation (Salehi *et al*., 2017).

Geopolymers have a high potential for use as new inorganic coatings to protect marine structural concrete, that is exposed to corrosion (Balan-Ortiz *et al*., 2017). Geopolymer coatings were applied to the concrete, bonding strongly within 4 h and resisting the shock of the sea waves. In addition, it was observed that the atmospheric humidity and the coating thickness are significant factors affecting the conservation of the layers (Zhang *et al*., 2012). The excellent anti-corrosive properties of geopolymers in seawater and their efficient bonds that harden the cement paste depend on the chemical composition of the geopolymer and its microstructure. A compact geopolymer is difficult for seawater to penetrate. The gel geopolymers of amorphous aluminosilicates were stable to seawater and air and provide sustainable protection for marine concrete structures (Zhang *et al*., 2010).

The behavior of mortars, hybrid geopolymers, alkaline ash and metakaolin compounds as protectors against chlorine corrosion in reinforced concrete has been studied, and the results show that metakaolin-based geopolymers exhibit the best behavior after five test cycles of humidity and drying (Aguirre-Guerrero *et al*., 2017). Infrastructure rehabilitation represents a great economic opportunity for the construction industry in the United States since the value of the industry is projected to exceed 1.6 trillion dollars during the next 5 years. The low-cost rehabilitation of concrete, including surface treatment has been reviewed and the use of geopolymers and their limitations were discussed in research by Pacheco-Torgal *et al*. (2012).

An insulating, heat-reflective coating was fabricated using a geopolymer made mainly of sodium silicate, metakaolin, sericite powder, talc, TiO_2, and glass microspheres as filler. This coating is inorganic,

environmentally friendly, resistant to water retention, and compact. In paint form, it has high durability, excellent dirt resistance, high reflectivity and good heat insulation. The results indicate that 12% TiO_2 and 6% glass microspheres will form the coating (Zhang *et al*., 2015a; Zhang *et al*., 2015b). Geopolymer-based coatings have a good inhibition to fire, are resistant to temperature and have anticorrosive properties. A coal ash-based geopolymer coating was studied using two variables, namely, the sodium-aluminum ratio and water-solid ratio, to observe the effect of the geopolymer's chemical composition on adhesion strength, setting time, microstructure and thermal stability at 800 °C. For this geopolymer, the maximum adhesion strength was 3.8 MPa with a sodium-aluminum ratio of 1 and a water-solid ratio of 0.33. The geopolymer formulations were thermally inactive up to 800 °C with a mass loss of 11 to 12% by dehydroxylation (Khan *et al*., 2015; Aziz *et al*., 2016).

The geopolymers containing metakaolinite and sodium silicate present good stability to leaching, freeze-thaw cycles, treatments at high temperatures and mechanical properties. Tension tests show excellent adhesion strength in the manufacturing of clay brick; the tensile strength of the geopolymer was 4.8 ± 0.8 MPa (Tamburini *et al*., 2017). The material most commonly used for geopolymer synthesis is metakaolinite resulting from the dehydroxylation of kaolinite (Osornio-Rubio *et al*., 2016). Metakaolinite is mixed with an alkaline activator such as sodium silicate, which causes it to quickly consolidate, forming a rigid material similar to traditional cement but with higher compressive strength (Khater, 2013).

Geopolymers were characterized based on their different uses, taking advantage of the large quantities of low-cost clays in Guanajuato state, Mexico. A geopolymer was obtained to be used as an internal coating in fixed kilns made of brick, or to repair concrete or for use in buildings as fire protection, given that it resists ignition up to 1000 °C.

2 Materials and methods

2.1 Clay sampling

The clays were previously selected for their refractory characteristics from different clay reservoirs located in the municipality of Comonfort, Guanajuato, Mexico (geographical coordinates: 20°43'7" North, 100°53'26" West); we have locally identified them as Caolín, Tepozán, and Bauwer. These reservoirs contain approximately 1 million tonnes of clay (Osornio-Rubio *et al*., 2016). For sampling, we used the methodology described in the NMX-AA-132-SCFI-2006 Mexican standard, where *in situ*, we marked a 1-m-spaced mesh. Next, random sampling in a quincunx pattern was performed. At each sampling point, 1 kg of clay was selected until 100 kg of sample per clay reservoir was reached.

2.2 Determination of moisture and calcination losses in clays

The clays were carefully pulverized in porcelain mortar to obtain a fine powder and 1 gr of each clay sample were taken and placed in previously tared porcelain crucibles. The crucibles were placed in an oven FELISA FE-291D (FELISA, Mexico) at 110 °C for 24 h. Subsequently, the samples were collocated in a desiccator. When the crucibles reached room temperature, they were weighed on an analytical balance Sartorius Model BL120S (Sartorius, Germany). To determine the losses by calcination, the samples were placed in a muffle furnace NOVATECH MD-20 (NOVATECH, Mexico) and calcined at 500 °C for 24 h. After cooling down to room temperature in a desiccator, the samples were weighed in analytical balance. This methodology was repeated to determine the losses by calcination at 1000 °C.

2.3 Chemical characterization of clays

Energy dispersive X-ray spectroscopy (EDS)

The initial identification of elemental composition in clay samples was performed with energy dispersive X-ray spectroscopy (EDS) using a JEOL JEM-100CX TEM (JEOL Ltd., Tokyo, Japan). The mineralogy of the raw clays was determined by powder X-ray diffraction (PXRD) with a Bruker D8 Advance instrument with a CuKα anode radiation (Bruker Corporation, Massachusetts, USA) in the range of $2\theta = 5 - 80^{o}$ using Bragg-Brentano geometry. The mineralogical characterization was performed with the MDI-JADE software version 6 (Materials Data, CA, USA).

Atomic absorption spectroscopy (AAS)

We used AAS to quantitatively determine the chemical composition in clays. For this study 0.5 gr of clay sample was weighed and mixed with a flux of lithium metaborate and lithium tetraborate (1:3 clay/flux ratio) in a platinum crucible and fused in a

muffle FELISA model FE-360 (FELISA, Mexico) at 900 °C for 1 h. Later, an extraction was carried out with a 10% w/w nitric acid solution. The extracted solution was placed in a 250 mL volumetric flask, gauging with the 10% w/w nitric acid solution (Torres-Ochoa, 2013). Calibration curves were constructed for the different metal oxides to be analyzed: SiO_2, Al_2O_3, CaO, MgO, Fe_2O_3, K_2O, Na_2O; for all these elements, standards for HYCEL atomic absorption of 1000 mg/ mL were used. The results were reported as % w/w of the metal oxide. For this study a Perkin Elmer AA200 atomic absorption spectroscope was used (Perkin Elmer, Waltham, MA, USA)

UV-VIS spectrophotometry

To validate the SiO_2 results, we used the silicomolybdate technique, which consists of reacting a sample of soluble silica $(SiO_4)^{-4}$ with molybdate ions $(MoO_4)^{-2}$ to form a complex of yellow color that is read at a wavelength of 650 nm using a spectrophotometer HACH DR/2000 (HACH, Loveland, CO, USA) with glass cell (Torres-Ochoa, 2013).

2.4 Experimental design

An important property of experimental design is the quantification of the change in response, which enables understanding the effects of changing the proportions of the individual mixture components, not only by changing the amount of sample. In mixture experiments, factors are the components or ingredients of a mixture, so the levels or quantities are not independent. Therefore, the sum of the proportions of the factors always gives the total mixture (Eqs. 1 and 2).

$$0 \le x_i \le 1, i = 1, 2, \ldots, p \quad (1)$$

$$x_1 + x_2 + \cdots + x_p = 1 \quad (2)$$

The mathematical models often used in mixture experiments are shown in Eqs. (3)-(6).

Linear

$$E(y) = \sum_{i=1}^{p} \beta_i x_i \quad (3)$$

Quadratic

$$E(y) = \sum_{i=1}^{p} \beta_i x_i + \sum \sum_{i<j}^{p} \beta_{ij} x_i x_j \quad (4)$$

Full Cubic

$$E(y) = \sum_{i=1}^{p} \beta_i x_i + \sum \sum_{i<j}^{p} \beta_{ij} x_i x_j + \sum \sum_{i<j}^{p} \delta_{ij} x_i x_j (x_i - x_j) + \sum \sum_{i<j<k} \sum \beta_{ijk} x_i x_j x_k \quad (5)$$

Special Cubic

$$E(y) = \sum_{i=1}^{p} \beta_i x_i + \sum \sum_{i<j}^{p} \beta_{ij} x_i x_j + \sum \sum_{i<j<k} \sum \beta_{ijk} x_i x_j x_k \quad (6)$$

In Eqs. (3)-(6), the parameter β_i represents the expected response according to a linear mixing rule. The second term, β_{ij}, in the equations is known as the linear mixing ratio. The quadratic and higher-level models predict curvature; in this case, positive values of β_{ij} represent synergistic behavior (which improves the response variable) while negative values of β_{ij} represent antagonistic behavior (which decreases the response variable). The response surface methodology is a set of tools to formulate a mathematical model with the objective of optimizing the response variable (Montgomery, 2012; Herrera-Franco *et al*., 2016).

2.5 Experimental design for geopolymer formulation

Previous studies have identified that sodium silicate can only be used in mixture proportions between 50-55%. When this proportion of sodium silicate is greater than 55%, the mixture becomes very liquid (due to the nature of the sodium silicate solution), making the formulated mortar difficult to handle and apply. On the other hand, when sodium silicate is less than 50% of the clay mixture (due to its adsorbent nature), it makes mixing difficult, preventing proper preparation of the mortar (Torres-Ochoa, 2013).

To develop the geopolymer, we used a simplex centroid experimental strategy for mixtures (Felix *et al*., 2018) considering the factors as a percentage of Caolín (C), Tepozán (T), and Bauwer (B), maintaining a constant concentration of sodium silicate (50%). The experimental design constraints were: Caolín 40% to 60%; Tepozán 40% to 60%, and Bauwer 0% to 20%. These restrictions represent the proportion of each pure clay powder, as obtained from previous experimental evidence (Torres-Ochoa, 2013).

Table 1. Compositions (%) of Caolín, Tepozán and Bauwer clays for geopolymer formulation at 50% w/w of sodium silicate.

Test	Sodium silicate	Caolín	Tepozán	Bauwer
1	50.0	30.0	20.0	0.0
2	50.0	20.0	30.0	0.0
3	50.0	20.0	20.0	10.0
4	50.0	25.0	25.0	0.0
5	50.0	25.0	20.0	5.0
6	50.0	20.0	25.0	5.0
7	50.0	23.3	23.3	3.4
8	50.0	26.7	21.7	1.6
9	50.0	21.7	26.7	1.6
10	50.0	21.7	21.7	6.6

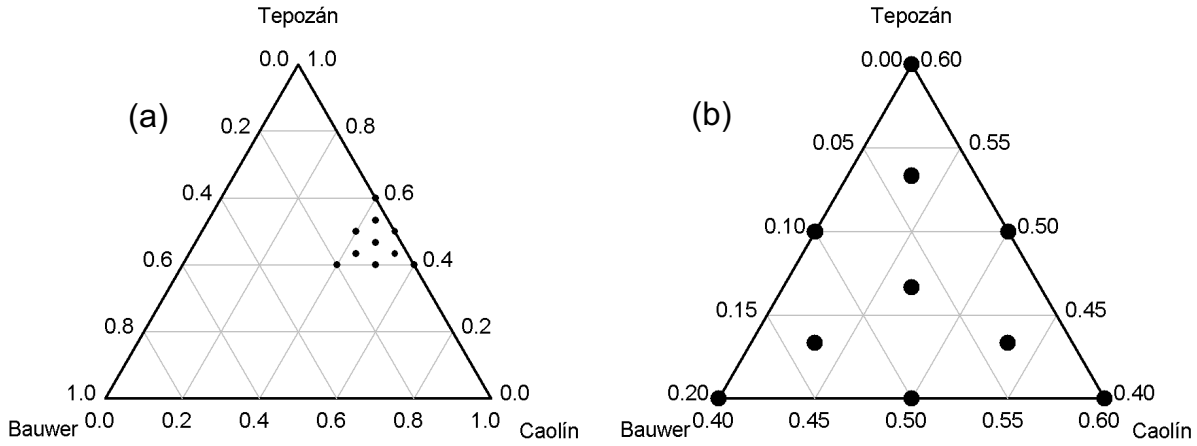

Fig. 1. Ternary diagram of the (a) complete graphic diagram of the feasible area, and (b) experimental design.

To form the geopolymer, the clays are blended to yield a homogeneous mixture. Fig. 1 shows the STATISTICA® v 8.0 ternary diagram for the clay mixture and region used, as well as the feasible region in which we carried out the experiments.

Table 1 shows the guideline for geopolymer development with 50% sodium silicate as the consolidating material (Vegmar Pinturas, Celaya, Mexico). The geopolymers were prepared with an electric mixer (GONI model 2708, CDMX, Mexico), first adding the proportion of sodium silicate solution and then the clay proportions, stirring up constantly for 5 min until the mixture became homogeneous.

2.6 Determining the adhesion of the geopolymer to red brick

Bricks with an attached 5 mm geopolymer layer were dried for 7 days and then cured at 1000 °C for 8 h in a muffle NOVATECH MD-20 (NOVATECH, Mexico). Fig. 2 shows the cured bricks without and with the geopolymer coating. The NMX-C-082-ONNCCE-2013 Mexican standard was used as a reference to measure the bond strength, using an array of red bricks each measuring 6 cm × 6 cm × 12 cm. The bricks were bonded with geopolymer as shown in Fig. 3.

The bond strength test was performed in a universal testing machine (Galdabini, Italy), and the result was applied to Eq. 7, where F is the fracture force measured in kg_f and S is the contact area among the three bricks, which is equal to 96 cm^2. Substituting the values in Eq. (7) resulted in the bond strength A in kg_f/cm^2.

$$A = \frac{F}{S} = \frac{F}{96\ cm^2} = [kg_f/cm^2] \quad (7)$$

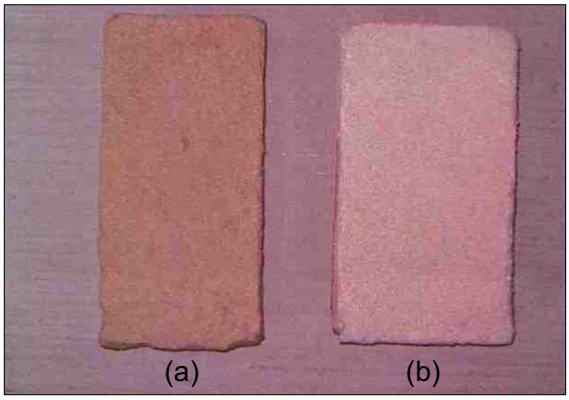

Fig. 2. Red clay bricks with thermal treatment at 1000 °C for 8 h, (a) without and (b) with geopolymer coating.

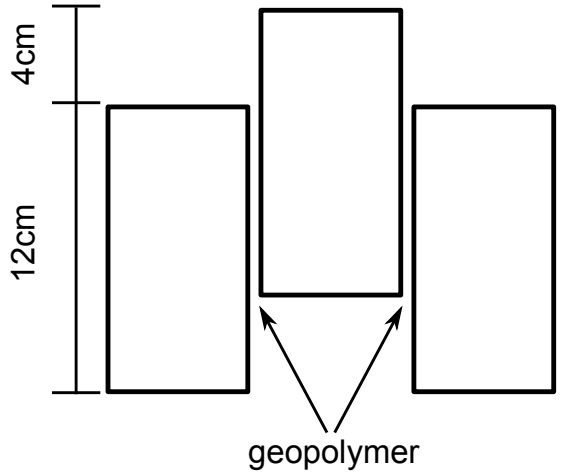

Fig. 3. Brick arrangement for the adhesion test according to NMX-C-082-ONNCCE-2013 Mexican standard.

2.7 Transmission Electron Microscopy (TEM)

The geopolymer samples were dispersed over isopropyl alcohol for 60 min in an ultrasonic bath, and then a drop was deposited on the cells using a micropipette. The TEM (JEOL, model JEM-1010 operated at 80 kV) micrographs were captured by a computer.

2.8 Thermogravimetric and Differential Thermal Analysis (TG/DTA)

Thermogravimetric and differential thermal analysis of the clays and the geopolymer was performed on a NETZSCH STA 409 (Netzsh Group, Bavaria, Germany) under atmospheric conditions with temperature ramp of 10 ºC/min over the range of 25-1000 ºC.

3 Results and discussion

3.1 Chemical characterization

Table 2 shows the mass percentages of the compounds analyzed by EDS, AAS, and UV-VIS, the moisture in the clays and the loss mass by calcination at 500 ºC and 1000 ºC.

Table 2. Chemical characterization of Caolín, Tepozán and Bauwer clays.

Compound	Tepozán	Caolín	Bauwer
SiO_2	62.76	47.90	68.13
Al_2O_3	22.06	28.33	6.78
CaO	0.31	0.38	0.32
MgO	0.54	0.49	9.29
Fe_2O_3	0.82	0.22	0.61
Na_2O	0.23	0.48	0.39
K_2O	0.22	2.98	0.12
$\%H_2O$	1.95	0.32	7.12
% Calcination losses (500 ºC)	1.58	1.20	2.75
% Calcination losses (1000 ºC)	9.42	17.69	3.82

Table 3. Mineralogical composition (% w/w) for Caolín, Tepozán and Bauwer clays.

Mineral Phase	Tepozán	Caolín	Bauwer
Kaolinite $Al_2Si_2O_5(OH)_4$	55.85	47.21	9.57
Alunite $KAl_3(SO_4)_2(OH)_6$	1.94	26.23	-
Quartz SiO_2	41.25	26.22	65.14
Smectite (Stevensite) $(Ca,Mg)_xMg_6Si_6O_{20}(OH)_{4\cdot n}H_2O$	-	-	18.17
Water	0.93	0.32	7.12

Silicon oxide (SiO_2) is the major component of all the clays, followed by aluminum oxide (Al_2O_3) for Tepozán and Caolín clays and magnesium oxide (MgO) for Bauwer clay. Calcium oxide (CaO), ferric oxide (Fe_2O_3), potassium oxide (K_2O), and sodium oxide (Na_2O) are found in smaller quantities in all the clays. In addition, the water absorbed by the clays from humid environments has a significant proportion in Bauwer clay at 7.12%, followed by Tepozán clay at 1.95%, and Caolín clay at 0.32%. In the case of calcination losses at 500 °C, one can observe that Bauwer clay exhibits a highest mass loss and Caolín clay has the lowest. For calcination losses to 1000 °C, the Caolín clay has the highest mass decrease while Bauwer clay has the lowest. Osornio-Rubio *et al*. (2016) compared clay compositions with others reported in the literature.

Table 3 shows the mineralogical composition for the three clays studied, with the results obtained from the chemical and mineralogical characterizations.

The Tepozán clay has the highest kaolinite content while Bauwer clay exhibits the lowest. Caolín clay has a significant proportion of alunite and Tepozán clay has alunite as a minority mineral. Bauwer clay has the highest quartz content and also contains a significant amount of stevensite. As Bauwer clay has a significant amount of smectite, and this mineral can absorb water in the interlaminar space, the high percentage of water is justified due to the atmospheric humidity and porosity according to the adsorption isotherms of these studied clays (Torres-Ochoa, 2013; Osornio-Rubio, 2016). The presence of kaolinite in the three clays is significant because it indicates their potential use in refractory materials manufacturing (Osornio-Rubio *et al*., 2016).

3.2 Geopolymer formulation

Table 4 shows the results for geopolymer adhesion to the red brick with a replicate, for a curing time of 7 days and a curing cycle at 1000 °C for 8 h. From the experimental results described in Table 4, we used the response surface methodology for developing the mathematical model for predicting the adhesion. Table 5 shows the statistical parameters for three least-squares models. The F-test value for the quadratic model is equal to 31.23, with an error probability of 0.31%; this is considered the best fit (Menezes *et al*., 2009; Navarrete-Bolaños *et al*., 2003) and has an R^2 of 0.9785 with an adjusted difference (R^2 - Ra^2) of 0.0269. Fig. 4(a) shows the ternary contour plot of the geopolymer adherence results on red clay bricks, and Fig. 4(b) shows the response surface for geopolymer adhesion to red clay bricks with a formulation using 50% commercial sodium silicate (Vegmar Pinturas, Celaya, Mexico) as the consolidating material.

Since the quadratic model probability is less than the 5% significance level, a statistically significant adhesion relationship exists for the formulated geopolymer.

Equation (8) shows the response surface quadratic model. If the parameters β_{ij} for interactions between the components are positive or negative, the effects of mixing components can be interpreted as synergistic or antagonistic (Solvason *et al*., 2009).

$$A(C,T,B) = -164.809\cdot C - 144.968\cdot T - 511.562\cdot B + 710.631\cdot C\cdot T + 846.313\cdot C\cdot B + 894.722\cdot T\cdot B \quad (8)$$

where A represents the adhesion (kg_f/cm^2), T is the Tepozán fraction, C is the Caolín fraction, and B is the Bauwer fraction.

The critical values that maximize the response surface are T = 0.4246, C = 0.4603, and B = 0.1150, with a predicted adhesion of 32.06 kg_f/cm^2. Based on this result, we formulated a geopolymer with the proportions (w/w): Caolín 21.0%, Tepozán 23.0%, Bauwer 6.0%, and consolidating agent 50.0%.

Following the same preparation methodology, and using three replicates for the geopolymer on red clay bricks, the following results were obtained for

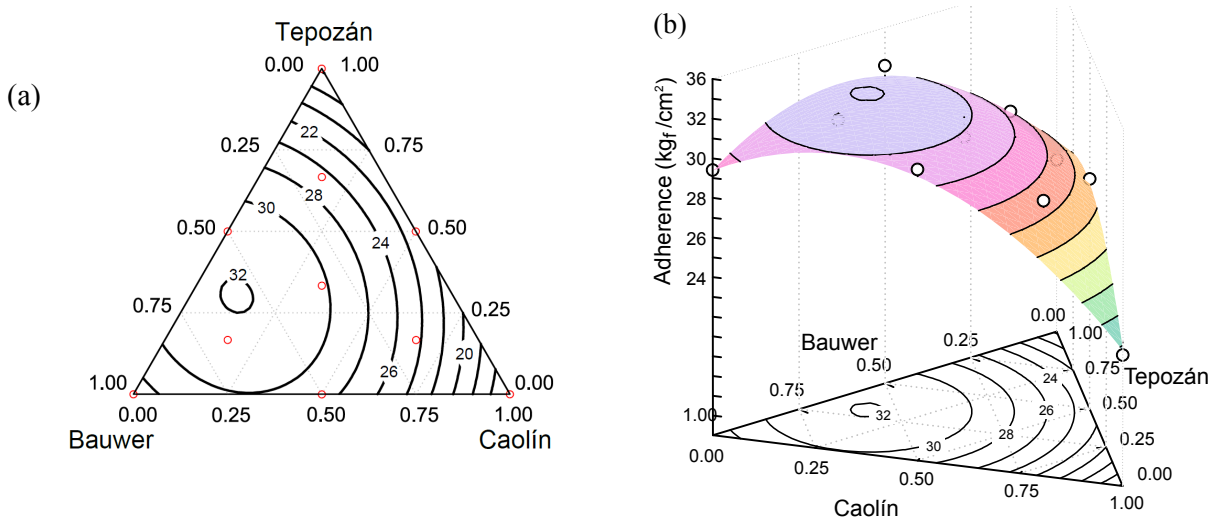

Fig. 4. (a) Ternary contour plot for adhesion in kg_f/cm^2. (b) Response surface with the quadratic model for adhesion.

Table 4. Geopolymer adhesion tests using the NMX-C-082-ONNCCE-2013 Mexican standard.

Test	Force Test 1 (kg_f)	Force Test 2 (kg_f)	Adhesion Test 1 (kg_f/cm^2)	Adhesion Test 2 (kg_f/cm^2)
1	902.4	1632.0	9.4	17.0
2	1324.8	2025.6	13.8	21.1
3	2256.0	2889.6	23.5	30.1
4	2073.6	2390.4	21.6	24.9
5	2572.8	3072.0	26.8	32.0
6	3004.8	3168.0	31.3	33.0
7	2246.4	3196.8	23.4	33.3
8	2256.6	2611.2	23.5	27.2
9	2371.2	2745.6	24.7	28.6
10	2496.0	3446.4	26.0	35.9

adhesion in a mechanical test: 27.15, 30.4, and 26.8 kg_f/cm^2, with an average of 28.11 kg_f/cm^2 (2.8 MPa) *versus* 32.06 kg_f/cm^2 (3.2 MPa) predicted.

3.3 Transmission electron microscopy (TEM) analysis

Fig. 5 shows the TEM micrographs for the consolidated geopolymer and thermally consolidated material at 1000 ºC. For the consolidated geopolymer, sodium silicate (SS, micrographs a and b) surrounds the structures of kaolinite (C, micrograph a) and quartz (Q, micrograph b). Based on this phenomenon, sodium silicate may bind to mineral phases forming larger and more complex structures. In micrograph c, the alumina (Al) are bound to a tridymite matrix. In micrograph d, alumina (Al) binds to a more complex structure, probably tridymite.

In micrograph e, the Al-Si spinel (Sp) phase is joined to an alumina structure (Al) and a tridymite (T) structure. Micrograph f shows (Sp) joined to one (Al) and a mullite.

Fig. 6(a) shows the results of thermogravimetric and differential thermal analysis in which Bauwer clay loses more moisture, a result congruent with that shown in Table 2. A common endothermic process is observed in the region of 480-680 °C (543.3 ºC for Bauwer, 563.3 ºC for Tepozán and 566.4 ºC for Caolín, the shadow zone in Fig. 6(a) associated with the dehydroxylation of kaolinite and alunite and their

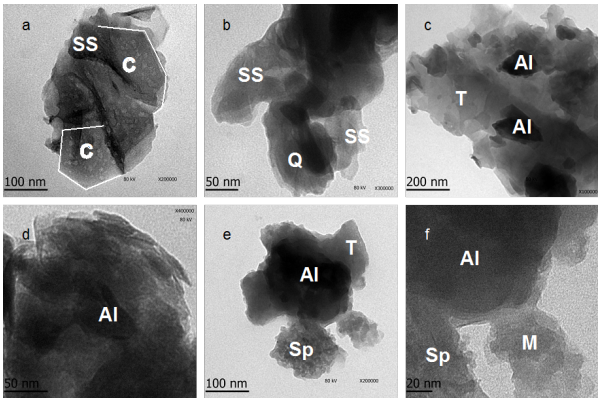

Fig. 5. TEM micrographs for (a, b) the consolidated geopolymer and (c to f) thermally consolidated at 1000 ºC. Identified mineral phases: sodium silicate (SS), kaolinite (C), quartz (Q), alumina (Al), tridymite (T), Al-Si spinel (Sp) and 2:1 mullite (M).

transformation into metakaolinite and meta-alunite, respectively. The presence of kaolinite in the three clays is significant because it indicates their potential use in refractory materials manufacturing and for common kaolinite applications in general (Osornio-Rubio *et al*., 2016; Peys *et al*., 2016). The second peak of the Caolín clay at 780.4 ºC is associated to the desulfation of alunite and corresponds to SO_3 release and the formation of amorphous Al_2O_3 (Frost and Wain, 2008; Kristóf *et al*., 2010).

The formulated geopolymer was also analyzed by TG/DTA as shown in Fig. 6(b). The geopolymer undergoes a common dehydration process to 93.7 ºC, based on the amount of water contained in the sodium silicate and the processes of the clays used as raw material. However, it does not have the endothermic process at 780.4 ºC corresponding to the desulphation of alunite. The geopolymer with 1000 ºC thermal treatment was analyzed to verify that it absorbs less than 1% of the ambient humidity; therefore, the thermal treatment confers stability to the formulated geopolymer.

Sodium silicate generates heat-insulating coatings when a geopolymer is formed (Zhang *et al*., 2015b; Zhang *et al*., 2015a). Geopolymers containing sodium silicate are stable to high-temperature treatments and have a tensile strength of 4.8 MPa (Tamburini *et al*., 2017).

The particle size of the clays used to form the geopolymer was 235 μm, which is within the 150-710 μm range that Kovárik *et al*. (2017) used to find stable geopolymers when exposed to 1000 °C. The obtained adhesion result (2.8 MPa) is comparable to the work of Zhang *et al*. (2015a) at 2.4 MPa.

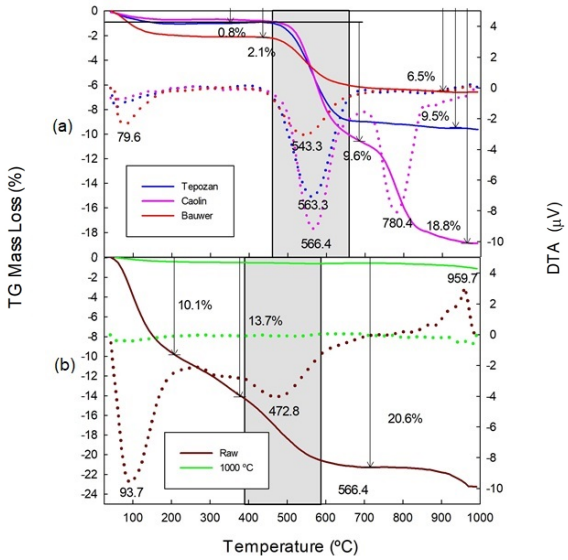

Fig. 6. (a) TG/DTA study of Caolín, Tepozán and Bauwer clays (solid lines represent the mass loss percentages, and the dotted lines represent the DTA curves), (b) formulated geopolymers before (raw) and after heat treatment at 1000 °C.

These authors analyzed different geopolymer formulations with fly ash and metakaolinite, measuring the adhesion to building material.

Also, Rego *et al*. (2014) reported a tensile strength of about 1 MPa for geopolymer stuck tiles. Geopolymers containing Na and Al have been studied to find an adhesion strength of 3.8 MPa that remains constant for temperatures up to 800 °C (Khan *et al*., 2015).

Table 5. Analysis of variance for the experimental design of geopolymer formulation.

Regression Model	SSR	DF	RMS	DF	DF	MSE	F-test	p-value	R^2	Adjusted R^2
Linear	152.5619	2	76.2809	168.6753	7	4.9088	3.17	0.1049	0.4749	0.3249
Quadratic	161.7681	3	53.9228	6.9067	5	1.3149	31.23	0.0031	0.9785	0.9516
Special Cubic	4.2484	1	4.2484	2.6583	3	0.9414	4.79	0.1163	0.9917	0.9752

SSR: sum of squares regression, DF: degrees of freedom, RMS: regression of the mean square, SSE: sum of squared errors, MSE: mean square error, R^2: Correlation coefficient.

In our investigation, sodium silicate-based geopolymers and clays with a high kaolinite percentage resisted thermal treatment up 1000 °C with tensile strength (adhesion) between the geopolymers and the red clay brick of 2.8 MPa, which is on the same order as results presented by Tamburini *et al*. (2017), and Khan *et al*. (2015). From the results of mineralogical composition described in Table 3, the raw geopolymer contains 23.33% kaolinite, 5.95% alunite, 18.90% quartz, 1.09% smectite, 0.71% water and 50.00% sodium silicate. The high proportions of kaolinite and quartz favor the fabrication of refractory materials (Osornio-Rubio *et al*., 2016).

Clays have the potential to synthesize high-quality geopolymers due to their high percentage of SiO_2 (Faris *et al*., 2017). In addition, Si and Al enable the geopolymers to have good morphology and link strength (Salehi *et al*., 2017). Their high kaolinite and alunite contents give them the potential to form refractory geopolymers. The dehydroxylation of kaolinite and its transformation into metakaolinite, as well as the dehydroxylation of alunite and its consequent transformation into meta-alunite are followed by a change in the coordination of the octahedral Al from Al^V to a combination of Al^{IV} and A^V (Osornio-Rubio, 2016), which allows the Al^{IV} and Al^V to join with sodium silicate to form a refractory geopolymer with good adhesion. Therefore, the geopolymer can be used for coatings due to its high adhesion strength and as a heat-resistant refractory material up to 1000 °C.

Conclusions

The chemical and mineralogical characterization by EDS, AAS, UV-VIS, PXRD and TG/DTA revealed that the raw material clays contain an important proportion of kaolinite and quartz, suggesting their potential use as a refractory material due to their high SiO_2 and Al_2O_3 composition. The adhesion experiments using a geopolymer formulated with 50% sodium silicate, 21% Caolín clay, 23% Tepozán clay and 6% Bauwer clay applied to red brick yielded a maximum adhesion strength of 28.11 kg_f/cm^2 (2.8 MPa). This value favors the use of the geopolymer as a red brick adhesive, but its applications are not limited to use on red clay bricks, since recent geopolymer applications have expanded.

Our results present values that favor the use of the geopolymer as a red clay coating, in particular, an internal coating during construction of brick burner kilns. By coating the internal wall of the furnace with refractory geopolymers, the furnace does not expand with its curing cycles at 1000 °C, since the geopolymer has good adhesion while resisting high temperatures.

It is also feasible to use this geopolymer as a coating for tiles and other ceramic materials that have thermal processing at temperatures up to 1000 ºC before their final use, as well as to reinforce or replace concrete exposed to high temperatures. The low cost of the clays in the community will allow the manufacture of cheap geopolymers that do not pollute by not generating CO_2 in their process, resulting in a community development opportunity for Delgado de Abajo, Comonfort Guanajuato, Mexico.

Acknowledgements

We gratefully acknowledge the financial support of CONCYTEG, Grant 08-09-k662-084. This study was carried out in the microscopy unit of the UNAM-Juriquilla. We also appreciate the support of Tecnológico Nacional de México (TecNM).

Abbreviations

AAS	Atomic Absorption Spectroscopy
EDS	Energy dispersive X-ray spectroscopy
PXRD	Powder X-ray Diffraction

TEM	Transmission Electron Microscopy
TG/DTA	Thermogravimetric and differential Thermal Analysis
UV-VIS	Ultraviolet-Visible Spectrophotometry

References

Aguirre-Guerrero, A., Robayo-Salazar, R.A. and Mejía de Gutiérrez, R. (2017). A novel geopolymer application: Coatings to protect reinforced concrete against corrosion. *Applied Clay Science 135*, 437- 446. DOI: 10.1016/j.clay.2016.10.029

Alshaaer, M., El-Eswed, B., Yousef, R.I., Khalili, F. and Rahier, H. (2016). Development of functional geopolymers for water purification, and construction purposes. *Journal of Saudi Chemical Society 20*, S85-S92. DOI: 10.1016/j.jscs.2012.09.012

Ankur, M. and Rafat, S. (2016). An overview of geopolymers derived from industrial by-products. *Construction and Building Materials 127*, 183-198. DOI: 10.1016/j.conbuildmat.2016.09.136

Aziz, I.H., Abdullah, M.M.A.B., Yong, H.C., Ming, L.Y., Hussin, J., Kadir, A.A. and Azimi, E.A. (2016). Manufacturing of fire resistance geopolymer: A review. *MATEC Web of Conferences 78*, 01023. DOI: 10.1051/matecconf/20167801023.

Balan-Ortiz, C.A., Luna Brito, M., Pérez López, T., and Camacho-Chab, R.J. (2017). Statistical analysis of electrochemical noise records obtained from the process of corrosion of reinforced steel embedded in concrete. *Revista Mexicana de Ingeniería Química 16*, 291-303.

Chang, T.-P., Shih, J.-Y., Yang, K.-M. and Hsiao, T.-C. (2007). Material properties of portland cement paste with nano-montmorillonite. *Journal of Materials Science 42*, 7478-7487. DOI:10.1007/s10853-006-1462-0

Clausi, M., Tarantino, S.C., Magnani, L.L., Riccardi, M.P., Tedeschi, C. and Zema, M. (2016). Metakaolin as a precursor of materials for applications in Cultural Heritage: Geopolymer-based mortars with ornamental stone aggregates. *Applied Clay Science 132-133*, 589-599. DOI: 10.1016/j.clay.2016.08.009

Duxson, P., Fernández-Jiménez, A., Provis, J.L., Lukey, G.C., Palomo, A.and Deventer, J.S.J. (2007). Geopolymer technology: the current state of the art. *Journal of Materials Science 42*, 2917-2933. DOI: 10.1007/s10853-006-0637-z

Faris, M.A., Abdullah, M.M.A.B., Sandu, AV., Ismail, K.N., Moga, L.M., Neculai, O. and Munjandy, R. (2017). Assessment of alkali activated geopolymer binders as an alternative of portlant cement. *Materiale Plastice 54*, 145-154.

Felix, A.C.S., Alvarez, L.D.G., Santana, R.A., Valasques Júnior, G.L., Bezerra, M.A., Neto, N.M.D., Lima, E.D., de Oliveira, A.A., Franco, M., and do Nascimento, B.B. (2018) Application of experimental designs to evaluate the total phenolics content and antioxidant activity of cashew apple bagasse. *Revista Mexicana de Ingenieria Química 17*, 165-175.

Frost, R.L. and Wain, D. (2008). A thermogravimetric and infrared emission spectroscopic study of alunite. *Journal of Thermal Analysis and Calorimetry 91*, 267-274. DOI: 10.1007/s10973-006-7979-2

Herrera-Franco, M.K.P., Hernández Fernández, F., and Valadez-González, A. (2016). Combined effect of an acrylic compatibilizer and two plasticizers on the tensile strength and strain of pla/starch blends using response surface methodology. *Revista Mexicana de Ingeniería Química 15*, 231-242.

Khan, M.I., Azizli, K., Sufian, S. and Man, Z. (2015). Sodium silicate-free geopolymers as coating materials: Effects of Na/Al and water/solid ratios on adhesion strength. *Ceramics International 41*, 2794-2805.DOI: 10.1016/j.ceramint.2014.10.099

Khater, H.M. (2013). Effect of silica fume on the characterization of the geopolymer materials. *International Journal of Advanced Structural Engineering 5*, 1-10. DOI: 10.1186/2008-6695-5-12

Kovárik, T., Rieger, D., Kadlec, J., Krenek, T., Kullová, L., Pola, M., Belský, P., France, P. and Říha, J. (2017). Thermomechanical

properties of particle-reinforced geopolymer composite with various aggregate gradation of fine ceramic filler. *Construction and Building Materials 143*, 599-606. DOI: 10.1016/j.conbuildmat.2017.03.134

Kristóf J., Frost R., Palmer S., Horváth E. and Jakab E. (2010). Thermoanalytical studies of natural potassium, sodium and ammonium alunites. *Journal of Thermal Analysis and Calorimetry 100*, 961-969. DOI: 10.1007/s10973-009-0581-7

Mehta A. and Siddique R. (2016). An overview of geopolymers derived from industrial by-products. *Construction and Building Materials 127*, 183-198. DOI: 10.1016/j.conbuildmat.2016.09.136

Menezes, R.R., Brasileiro, M.I., Gonçalves, W.P., Santana, L.N. de L., Neves, G.A., Ferreira, H.S. and Ferreira, H.C. (2009). Statistical design for recycling kaolin processing waste in the manufacturing of mullite-based ceramics. *Materials Research 12*, 201-209. DOI: 10.1590/S1516-14392009000200015

Montgomery, D.C. (2012). *Design and Analysis of Experiments*. John Wiley & Sons, Inc, Eighth Edition. Hoboken, NJ. USA.

Navarrete-Bolaños, J.L., Jiménez-Islas, H., Botello-Alvarez, E. and Rico-Martínez, R. (2003). Mixed culture optimization for marigold flower ensilage via experimental design and response surface methodology. *Journal of Agricukltural and Food Chemistry 51*, 2206-2211. DOI: 10.1021/jf0257650

NMX-AA-132-SCFI-2006. (2006). *Muestreo de Suelos para la Identificación y la Cuantificación de Metales y Metaloides, y Manejo de la Muestra* (In Spanish). Secretaria de Economía. México.

NMX-C-082-ONNCCE-2013. (2013). *Industria de la Construcción, Mampostería, Determinación de la Adherencia por Esfuerzo Cortante entre el Mortero y las Piezas de Mampostería Método de Ensayo*. (In Spanish). Organismo Nacional de Normalización y Certificación de la Construcción y Edificación S.C. México.

Osornio-Rubio, N.R. (2016). *Caracterización y Modificación de Arcillas Minerales y Estudio de su Uso en la Remoción de Cromo Hexavalente (CrVI)*. PhD Thesis (In Spanish). Instituto Tecnológico de Celaya. México.

Osornio-Rubio, N.R., Torres-Ochoa, J.A., Palma-Tirado, M.L., Jiménez-Islas, H., Rosas-Cedillo, R., Fierro-González, J.C. and Martínez-González, G.M. (2016). Study of the dehydroxylation of kaolinite and alunite from a Mexican clay with DRIFTS-MS. *Clay Minerals 51*, 55-68. DOI:10.1180/claymin.2016.051.1.05

Pacheco-Torgal, F., Abdollahnejad, Z., Miraldo, S., Baklouti, S. and Ding, Y. (2012). An overview on the potential of geopolymers for concrete infrastructure rehabilitation. *Construction and Building Materials 36*, 1053-1058. DOI: 10.1016/j.conbuildmat.2012.07.003

Perez-Monserrat, E.M., de Buergo, M.A., Gomez-Heras, M., Muriel, M.J.V. and Gonzalez, R.F. (2013). An urban geomonumental route focusing on the petrological and decay features of traditional building stones used in Madrid, Spain. *Environmental Earth Sciences 69*, 1071-1084. DOI: 10.1007/s12665-012-2164-3

Peys, A., Rahier, H. and Pontikes, Y. (2016). Potassium-rich biomass ashes as activators in metakaolin-based inorganic polymers. *Applied Clay Science 119*, 401-409. DOI: 10.1016/j.clay.2015.11.003

Rego, S.R., Gomes, K.C., Rosas, M., Torres, S.M. and de Barros, S. (2014). Application of geopolymeric adhesives in ceramic systems subjected to cyclic temperature environments. *The Journal of Adhesion 90*, 120-133. DOI: 10.1080/00218464.2013.794109

Salehi, S., Khattak, M. J., Bwala, A.H. and Karbalaei, F.S. (2017). Characterization, morphology and shear bond strength analysis of geopolymers: Implications for oil and gas well cementing applications. *Journal of Natural Gas Science and Engineering 38*, 323-332. DOI: 10.1016/j.jngse.2016.12.042

Solvason, C.C., Chemmangattuvalappil, N.G., Eljack, F.T. and Eden, M.R. (2009). Efficient visual mixture design of experiments using property clustering techniques. *Industrial & Engineering Chemistry Research 48*, 2245-2256. DOI: 10.1021/ie800877d

Tamburini, S., Natali, M., Garbin, E., Panizza, M., Favaro, M. and Valluzzi, M.R. (2017). Geopolymer matrix for fibre reinforced composites aimed at strengthening masonry structures. *Construction and Building Materials 141*, 542-552. DOI: 10.1016/j.conbuildmat.2017.03.017

Torres-Ochoa, J.A. (2013). *Síntesis de un Geopolímero Refractario: Estudio de un Proceso de Consolidación Térmica y su Aplicación como Recubrimiento Interno de Hornos Ladrilleros*. M.S. Thesis (in Spanish). Instituto Tecnológico de Celaya. México.

Yun-Ming, L., Cheng-Yong, H., Mustafa, M., Bakri, A. and Hussin, K. (2016). Progress in materials science structure and properties of clay-based geopolymer cements?: A review. *Progress in Materials Science 83*, 595-629. DOI: 10.1016/j.pmatsci.2016.08.002

Zhang Z., Yao X. and Wang H. (2012). Potential application of geopolymers as protection coatings for marine concrete III. Field experiment. *Applied Clay Science 67-68*, 57-60. DOI: 10.1016/j.clay.2012.05.008

Zhang Z., Yao X. and Zhu H. (2010). Potential application of geopolymers as protection coatings for marine concrete II. Microstructure and anticorrosion mechanism. *Applied Clay Science 49*, 7-12.DOI: 10.1016/j.clay.2010.04.024

Zhang, H.Y., Kodur, V., Qi, S.L. and Wu, B. (2015a). Characterizing the bond strength of geopolymers at ambient and elevated temperatures. *Cement and Concrete Composites 58*, 40-49. DOI: 10.1016/j.cemconcomp.2015.01.006

Zhang, Z., Wang, K., Mo, B., Li, X. and Cui, X. (2015b). Preparation and characterization of a reflective and heat insulative coating based on geopolymers. *Energy and Buildings 87*, 220-225. DOI: 10.1016/j.enbuild.2014.11.028